Quantum Repeaters with Automorphic CNOTs

Haoyan Lou
Rutgers University
Piscataway, USA
haoyan.lou@rutgers.edu

Allison Klingler
Amherst College
Amherst, USA
aklingler27@amherst.edu

Winston Li
Rutgers University
Piscataway, USA
wl605@scarletmail.rutgers.edu

Pooja Kedia
Rutgers University
Piscataway, USA
pk641@scarletmail.rutgers.edu

Enhyeok Jang
Yonsei University
Seoul, South Korea
enhyeok.jang@yonsei.ac.kr

Alexei Ashikhmin
Nokia Bell Labs
Murray Hill, USA
alexei.ashikhmin@nokia-bell-labs.com

Yipeng Huang
Rutgers University
Piscataway, USA
yipeng.huang@rutgers.edu

***Abstract*—Repeaters are a key building block for quantum networks, enabling long-distance entanglement between remote terminals. However, their performance may be limited by asymmetric noise induced by the remote CNOT (controlled NOT) protocol, where control and target qubits experience different dominant error types. This motivates the use of asymmetric quantum error-correcting codes in neighboring repeater stations. We first show that directly adopting such asymmetric code pairs is highly constrained. For asymmetric CSS code pairs matched to the remote-CNOT noise model, neither fully transversal nor partial transversal CNOT constructions can provide the desired logical CNOT while preserving the required asymmetric protection. To overcome this, we propose a repeater architecture based on asymmetric quantum Reed-Muller codes and automorphic logical CNOTs. Instead of implementing logical CNOTs across heterogeneous codes, we construct a larger distributed code through transversal remote CNOTs and realize the logical operation via qubit-permutation-based transformations within the code, thereby aligning error protection with the asymmetric noise structure. Our results show that the proposed asymmetric design can reduce the logical error rate induced by remote CNOTs over symmetric ones with the same physical qubit budget.**

I. Introduction

Repeaters are a building block for quantum networks, enabling long-distance entanglement between remote terminals. Such entanglement supports a wide range of new applications such as quantum cryptography [1], [5], [6], [11] and distributed quantum computing [3]. These systems rely on photonic channels for transmitting qubits, where losses and noise degrade the fidelity of transmitted quantum states exponentially with distance [22]. Quantum error correction can mitigate these effects and is an essential component of scalable quantum repeater architectures. Existing repeater designs typically employ identical symmetric quantum error-correcting codes at all repeater stations, where each node is encoded using the same code with equal capability to correct both X and Z errors. These designs fail to exploit the inherent asymmetric error introduced by the remote CNOT protocol used for entanglement distribution. In practice, the remote CNOT protocol propagates noise unevenly across control and target qubits, leading to a mismatch between the error model and the protection offered by identical symmetric codes. This observation motivates a repeater design that accounts for asymmetric noises. In this work, we propose a quantum repeater architecture based on asymmetric QRMs (quantum Reed-Muller codes [2], [21], [25]) and automorphic logical CNOTs, enabling neighboring repeater stations to have different error-correcting capabilities while still supporting fault-tolerant logical CNOT operations.

979-8-3195-0662-7/26/$31.00 ©2026 IEEE

II. Background and Motivation

Repeaters can divide a long-distance quantum network link into short segments [8], [10]. Although such repeaters were envisioned to operate on physical hardware qubits without error correction, the second generation of such repeaters uses quantum error correction codes (QECCs) [12], [14], [19], [23] to protect against noise in hardware and on photons [18]. As shown in Fig. 1, such repeaters need to perform 2 protocols, entanglement distribution and entanglement swapping, to establish entanglement between repeater A and C.

1) Entanglement distribution: The goal of entanglement distribution is to create entangled logical qubit pairs between two neighboring quantum repeaters by applying logical CNOTs. As was envisioned in the original second-generation quantum repeaters, each repeater implements separate blocks of the same CSS code [9], [20], so that logical CNOTs are implemented by transversal physical CNOTs. These physical CNOTs are done, in turn, via remote CNOTs from consuming entangled photonic qubits transmitted to the two repeaters [15] as illustrated in Fig. 2. The entangled photon pair in the remote CNOT protocol suffers depolarizing noises after creation. And these noises propagate to q_A, the control qubit, and q_B, the target qubit, differently. In detail, from the noise model in [15], the control qubit is more likely to suffer a Z error, and the target qubit is more likely to suffer an X error after the remote CNOT gate. The asymmetry motivates the design of a repeater architecture that can match the biased error model with the correction ability of two asymmetric codes.

2) Entanglement swapping: occurs in all intermediate repeaters after the entanglement distribution. In each intermediate repeater, there are always two sets of codes. Logical qubits of the first code are entangled to logical qubits in the

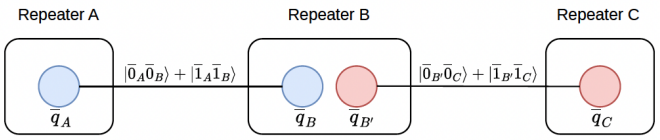

Fig. 1. Illustration of three repeaters. The goal is to entangle $\overline{q}_A$ in repeater A and $\overline{q}_C$ in repeater C, with repeater B in the middle. After entanglement distribution, $\overline{q}_A$ and $\overline{q}_B$ are entangled in the $|\overline{0}_A\overline{0}_B\rangle + |\overline{1}_A\overline{1}_B\rangle$ state, $\overline{q}_{B'}$ state and $\overline{q}_C$ are entangled in the $|\overline{0}_{B'}\overline{0}_C\rangle + |\overline{1}_{B'}\overline{1}_C\rangle$ state. To entangle $\overline{q}_A$ and $\overline{q}_C$, the next step is to perform entanglement swapping in repeater B.

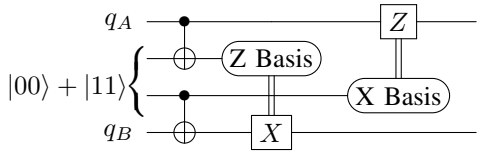

Fig. 2. Illustration of remote CNOT. In this figure, we have two physical qubits, q_A and q_B, that are far apart in two neighboring repeaters, and we want to perform a CNOT gate between them. The first step is to generate an entangled photon pair in the $|00\rangle + |11\rangle$ state. Then we send one photon to q_A and the other to q_B. And perform CNOT gates between the physical qubits and photons as shown in the figure. Finally, we measure photons in the Z and X bases and send the classical information of the measurement result to the other repeater to perform correction. The entire process effectively implements a CNOT gate between q_A and q_B using a pair of entangled photons.

previous repeater, and logical qubits of the second code are entangled to logical qubits in the next repeater. Then, we first perform Bell measurements between the logical qubits in the two codes in the intermediate repeater. After this, we send the readout results via classical communication to the previous and next repeaters to apply Z or X corrections. As a result, an entanglement is established between the logical qubits at the two ends of the network [7]. Fig. 3 shows the logical level operation that establishes an entanglement between repeater A and C with an intermediate repeater B.

III. Limitations on QECCs for 2nd Gen. Repeaters

Second-generation repeater proposals employ identical CSS codes in all repeater stations. In this setting, logical Bell-state preparation can be performed using transversal CNOTs [14], which are realized by applying physical CNOTs between all corresponding qubits in neighboring blocks. To better match the asymmetric noise arising from remote CNOTs, recent works have proposed the idea of employing different CSS codes in neighboring repeaters [4], [16], [24]. In [24], the potential performance advantages of asymmetric codes for quantum communication over asymmetric channels have been demonstrated. These do not address how asymmetric code blocks can be incorporated into a fault-tolerant repeater architecture. Our implementation in Sections IV and V provides, to the best of our knowledge, the only explicit architecture that allows asymmetric code pairs to be incorporated into a second-generation repeater protocol while still supporting these logical CNOT operations. The simulation results in Section VI show the benefit of this approach. For a fixed number of physical qubits per repeater, our asymmetric-code construction achieves

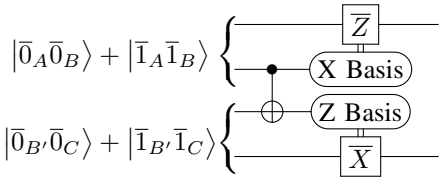

Fig. 3. Illustration of the entanglement swapping process. In this figure, the qubit on the top is $\overline{q}_A$ in repeater A, the qubit at the bottom is $\overline{q}_C$ in repeater C, and the two qubits in the middle are $\overline{q}_B, \overline{q}_{B'}$ in repeater B. After entanglement distribution, $\overline{q}_A, \overline{q}_B$ are entangled, and $\overline{q}_{B'}, \overline{q}_C$ are entangled. Now we measure $\overline{q}_B, \overline{q}_{B'}$ in the Bell basis and send the classical information of the measurement result to $\overline{q}_A$ and $\overline{q}_C$ to apply corrections. After the entire process, $\overline{q}_A, \overline{q}_C$ will be entangled in the $|\overline{0}_A\overline{0}_C\rangle + |\overline{1}_A\overline{1}_C\rangle$ state.

lower logical error rates than the corresponding symmetric-code baselines. Using asymmetric codes that satisfy the noise model with (partial) transversal CNOTs is a conventional approach. The central difficulty of this idea is ensuring that these codes can still support the logical CNOT operations required for entanglement distribution. We will show that most of such designs are impossible.

A. Asymmetric CSS code pair with fully transversal CNOTs

We hope to find a pair of asymmetric QECCs that satisfy the asymmetric noise of the remote CNOT gate. If we apply remote CNOTs from code A to code B, then we want code A with a higher d_Z and code B with a higher d_X. Thus, code A can better protect against Z errors while code B can better protect against X errors. Furthermore, it is required that remote fully transversal CNOTs from A as control to B as target result in logical CNOTs from A to B. However, as implied from Theorem 1 in [4], for two CSS codes, if the transversal CNOTs from code A to code B implement logical CNOTs from A to B, then we have $E_Z^A \subseteq E_Z^B$, where E_Z^A is the set of Z errors that can be corrected by code A and E_Z^B is the set of Z errors that can be corrected by code B. Thus, this approach does not work. It cannot provide better protection against biased remote CNOT noise than just using identical symmetric codes with the same number of physical qubits, which shows the limitation of [16].

B. Asymmetric CSS code pair with partial transversal CNOTs

The previous subsection rules out the most direct approach, where logical CNOTs between codes are implemented by fully transversal remote CNOTs. A natural relaxation is to allow only partial transversal CNOTs to be applied. However, we will prove that this relaxation is still not sufficient for the repeater setting considered here.

Definition 1. Let Q_A and Q_B be two $[[n,k]]$ quantum codes, where Q_A is the control code block and Q_B is the target code block. For a subset $S \subseteq \{1,\dots,n\}$ of physical-qubit indices, we define the partial transversal CNOT operator for the code pair (Q_A, Q_B) as $U_S = \prod_{i\in S} CX_i$, where CX_i denotes the physical CNOT acting from the i^{th} physical qubit of Q_A to the i^{th} physical qubit of Q_B. The code pair (Q_A, Q_B) admits partial transversal logical CNOTs if there exists a partial transversal CNOT U_S such that, on the code space,

$\prod_{j\in M}\overline{CX}_j = \prod_{i\in S} CX_i$, where $M \subseteq \{1,\dots,k\}$ is a subset of the k logical-qubit pairs encoded in (Q_A, Q_B), and $\overline{CX}_j$ denotes the logical CNOT from the j^{th} logical qubit of Q_A to the j^{th} logical qubit of Q_B. This operation preserves the original structure of the code pair (Q_A, Q_B) if it does not change the stabilizers of the two codes, and it acts as logical identities on logical qubits not in M.

Theorem 1. *If a $[[n,k,d]]$ CSS code pair (Q_A, Q_B), where Q_A is the control and Q_B is the target, has partial transversal logical CNOTs that preserve the original structure of (Q_A, Q_B), then $d_Z(A) \le d_Z(B)$. i.e. the Z distance of Q_A is smaller than or equal to the Z distance of Q_B.*

Proof. Since (Q_A, Q_B) has partial transversal logical CNOTs, we have $S \subset \{1,...,n\}, M \subseteq \{1,...,k\}$ s.t. $\prod_{j\in M}\overline{CX}_j = \prod_{i\in S} CX_i$. Each code has k equivalence classes of logical Z operators, $\overline{\mathbb{Z}}_{A,1},...,\overline{\mathbb{Z}}_{A,k}$ for Q_A and $\overline{\mathbb{Z}}_{B,1},...,\overline{\mathbb{Z}}_{B,k}$ for Q_B, where all the elements in $\overline{\mathbb{Z}}_{A,i}$ performs a equivalent logical Z operation on the i^{th} logical qubit in Q_A, similar for $\overline{\mathbb{Z}}_{B,i}$.

For the default construction of a CSS code, all the logical $\overline{Z}$ operations consist of only physical Z operations. Thus, for every logical $\overline{Z}_{B,i}$ operator in Q_B, there exists $P_{B,i} \subseteq \{1,\dots,n\}$ such that $\overline{Z}_{B,i} = \prod_{j\in P_{B,i}} Z_j$, where the product of the single-qubit Pauli operators Z_j forms the physical n-bit pure Z representative of the equivalence class $\overline{\mathbb{Z}}_{B,i}$. A Z type logical operation $\overline{Z}_B$ in Q_B is a product of some logical $\overline{Z}$ operations. Thus, a Z-type logical operator in Q_B can be expressed as follows: $\overline{Z}_B = \prod_{i\in H}\overline{Z}_{B,i} = \prod_{i\in H}\prod_{j\in P_{B,i}} Z_j$ for some $H \subseteq \{1,\dots,k\}$ and $P_{B,i} \subseteq \{1,\dots,n\}$. A logical operator is still in the logical equivalence class after being multiplied by stabilizers of the code. We consider an arbitrary representative of a logical $\overline{Z}$ operator for Q_B: $\overline{Z}^*_B = S_B\overline{Z}_B = S_B\prod_{l\in H}\prod_{j\in P_{B,l}} Z_j$, where S_B is an X-type stabilizer of code Q_B. Consider the Heisenberg picture operator of $\overline{Z}^*_B$ after the partial transversal logical CNOTs. We observe that

$$
\begin{aligned}
&\prod_{j\in M}\overline{CX}_j\big(\overline{I}^{\otimes k}\otimes\overline{Z}^*_B\big)\prod_{j\in M}\overline{CX}_j \qquad (1)\\
&= \prod_{i\in S} CX_i\big(I^{\otimes n}\otimes S_B\prod_{l\in H}\prod_{j\in P_{B,l}} Z_j\big)\prod_{i\in S} CX_i\\
&= \prod_{i\in S} CX_i\big(I^{\otimes n}\otimes S_B\big)\prod_{i\in S} CX_i\\
&\quad * \prod_{l\in H}\Big(\prod_{i\in S} CX_i\big(I^{\otimes n}\otimes\prod_{j\in P_{B,l}} Z_j\big)\prod_{i\in S} CX_i\Big)\\
&= \big(I^{\otimes n}\otimes S_B\big) * \prod_{l\in H}\big(\prod_{k\in S\cap P_{B,l}} Z_k\otimes\prod_{j\in P_{B,l}} Z_j\big)\\
&= \big(\prod_{l\in H}\prod_{k\in S\cap P_{B,l}} Z_k\big)\otimes S_B\big(\prod_{l\in H}\prod_{j\in P_{B,l}} Z_j\big). \qquad (2)
\end{aligned}
$$

In the logical level, formula (1) is also equivalent to $\overline{Z}^*_A\otimes\overline{Z}^*_B$. We assume that the partial transversal logical CNOTs preserve the original structure of (Q_A, Q_B). So the Z type logical operator of Q_A should act as the identity on qubits in Q_B and vice versa. We get a representation of $\overline{Z}^*_A$ from formula (2) as follows: $\overline{Z}^*_A = \prod_{l\in H}\prod_{k\in S\cap P_{B,l}} Z_k$. If we compute the weight of Z type physical operators of $\overline{Z}^*_A$ and $\overline{Z}^*_B$, we immediately get $w(\overline{Z}^*_A) \le w(\overline{Z}^*_B)$. If (Q_A, Q_B) has partial transversal CNOTs that preserve the original code structures, for every Z type logical operator $\overline{Z}^*_B$ of Q_B, we can always construct a Z type logical operator $\overline{Z}^*_A$ of Q_A with $w(\overline{Z}^*_A) \le w(\overline{Z}^*_B)$. By the definition of the Z distance, d_Z is the minimal weight of all logical Z operators of the code, or the number of qubits where the operator differs from I [13]. Now we can conclude that $d_Z(A) \le d_Z(B)$.

□

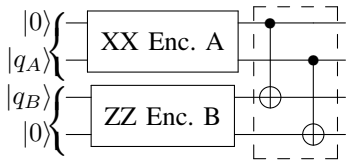

Fig. 4. Illustration of recursively constructing a $[[4,2,2]]$ code with a $[[2,1,1]]$ XX and a $[[2,1,1]]$ ZZ code. If we employ this architecture in quantum repeaters, the two different $[[2,1,1]]$ codes should be placed in the two neighboring repeaters separately, and the two physical CNOTs in the box will be replaced with remote CNOTs.

This leads to the same conclusion as the previous subsection, where the set of Z errors that can be corrected by code A must be a subset of the set of Z errors that can be corrected by code B. Asymmetric CSS codes with partial transversal logical CNOTs cannot work for the remote CNOT noise setting.

C. Asymmetric non-CSS code pair

We can also search for asymmetric non-CSS code pairs that support the required logical CNOT operations. Such codes are more general than CSS codes, but they lose the structural features that make the asymmetric repeater design tractable and scalable in this work. Therefore, while non-CSS asymmetric code pairs may be an interesting direction for future work, they are outside the scope of this paper.

IV. Asymmetric QRM Code for Remote CNOT Noise

Due to the limitations mentioned previously, we explore an alternative design philosophy that completely removes the requirement of logical CNOT transversality between neighboring repeaters. We temporarily combine neighboring asymmetric code blocks into a larger distributed code using transversal remote CNOTs. Logical CNOTs are then implemented via automorphisms of the larger code, with all SWAP gates realized via qubit relabeling. In this work, we focus on QRMs because they provide an explicit code family satisfying the two properties required by our approach.

A. Recursive construction to larger code families

We note that a pair of asymmetric QRMs can be entangled to form a larger one by applying transversal CNOTs from the one with higher d_Z (more X stabilizers) to the one with higher d_X (more Z stabilizers). $[[2,1,1]]$ XX code with stabilizer $S = \{XX\}$ and $[[2,1,1]]$ ZZ code with $S = \{ZZ\}$ can be combined into a $[[4,2,2]]$ code with $S = \{ZZZZ, XXXX\}$

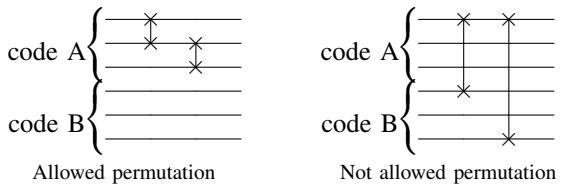

Fig. 5. Illustration of allowed and not allowed permutations that generate the logical CNOTs.

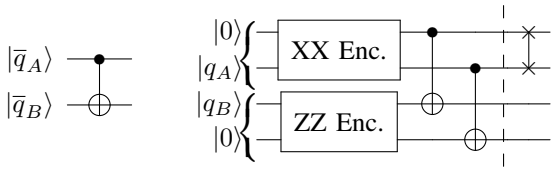

Fig. 6. Illustration of the automorphic logical CNOT in $[[4,2,2]]$ code, constructed from asymmetric $[[2,1,1]]$ codes. The right circuit is the physical implementation of the left logical CNOT gate in codeword space. Here, the physical SWAP gate can be implemented virtually by qubit relabeling.

via transversal CNOTs from XX code to ZZ code as shown in Fig. 4. If we implement the physical CNOTs using remote CNOTs, then the XX code provides stronger protection against the resulting Z errors, whereas the ZZ code provides stronger protection against the resulting X errors. QRM taxonomy can also provide more code families that meet these criteria. For the next larger case, one could consider a pair of asymmetric $[[8,3,2]]$ codes to form a $[[16,6,4]]$ code.

B. Automorphic logical CNOT by local relabelings

We find several larger codes constructed from asymmetric QRM pairs, with automorphic logical CNOT(s) between logical qubits that were originally in the different asymmetric codes. Relabelings are local to the control or target side of the code system. The logical CNOT in $[[4,2,2]]$ code can be realized by relabeling 2 qubits that are in $[[2,1,1]]$ XX code as shown in Fig. 6. The next larger one is the $[[16,6,4]]$ code constructed from asymmetric $[[8,3,2]]$ pair. But in this case, we will use only two logical qubits in each of the $[[8,3,2]]$ code, as we can only implement two logical CNOTs inside the $[[16,6,4]]$ code at a time by local qubit relabeling.

V. Error suppression via proposed architecture

The QRM pair discussed above can mitigate the asymmetric noise from the remote CNOTs. Let code A have a higher d_Z and code B have a higher d_X. These two codes are alternated along the entanglement distribution path, such that adjacent repeaters employ two different asymmetric codes. This ensures that, for each remote CNOT, the control qubit is encoded in a code with stronger protection against Z errors, while the target qubit is encoded in a code with stronger protection against X errors. All intermediate repeaters employ two identical codes, which simplifies entanglement swapping. The entanglement distribution between two neighboring repeaters is carried out according to the following steps: ① We construct a larger code by performing transversal remote CNOTs from the higher d_Z code to the higher d_X code. ② To implement the logical

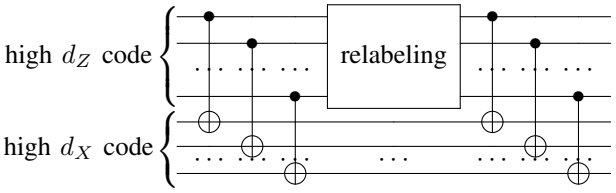

Fig. 7. Illustration of the general entanglement distribution process using our asymmetric codes with automorphic logical CNOTs design. Here, all the physical CNOT gates are implemented by remote CNOTs.

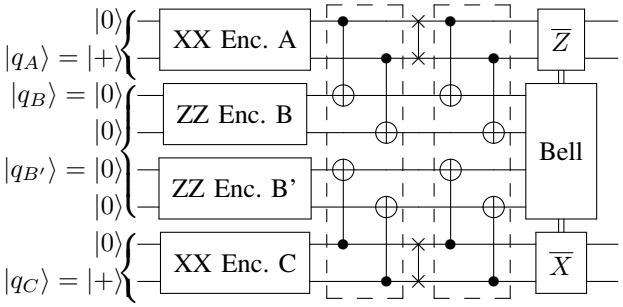

Fig. 8. Illustration of creating a logical entangled pair between repeater A and C via an intermediate repeater B using asymmetric $[[2,1,1]]$ codes.

CNOTs between the two closest repeaters, we apply qubit permutations within one repeater. This can be done at no physical cost using qubit relabeling. ③ Then, we decompose the larger code to recover the original code blocks by performing transversal remote CNOTs from the higher d_Z code to the higher d_X code. After this process, we can do the syndrome measurements within each repeater. Fig. 7 demonstrates the general process of the above steps.

Fig. 8 illustrates a repeater design for entangling the logical qubits in repeaters A and C via an intermediate repeater B, by encoding the logical qubits into the different $[[2,1,1]]$ codes at each repeater. The top two qubits reside in repeater A, the four intermediate qubits in B, and the bottom two qubits in C. All CNOTs enclosed in dotted-line boxes are implemented remotely. We encode $|q_A\rangle, |q_C\rangle$ to $[[2,1,1]]$ XX code A and code C, and encode $|q_B\rangle, |q_{B'}\rangle$ to $[[2,1,1]]$ ZZ code B and code B'. After the first layer of remote CNOTs, code A, B, and code B', C are combined into two $[[4,2,2]]$ codes. Then we perform qubit permutations acting only on the physical qubits within code A and code C. These permutations implement the logical CNOT$(|\overline{q}_A\rangle \to |\overline{q}_B\rangle)$ and CNOT$(|\overline{q}_C\rangle \to |\overline{q}_{B'}\rangle)$. Subsequently, we decompose the two $[[4,2,2]]$ codes back to the original $[[2,1,1]]$ XX and ZZ code pairs via another layer of remote CNOTs so that we can perform syndrome measurement locally within each repeater. Finally, we perform the entanglement swapping to entangle the logical qubits $|\overline{q}_A\rangle$ and $|\overline{q}_C\rangle$. Throughout this, the control qubits of all remote CNOTs are encoded in codes with higher d_Z, while the target qubits are encoded in codes with higher d_X.

The same design can be used if we replace the simple asymmetric $[[2,1,1]]$ codes with asymmetric $[[8,3,2]]$ codes, which can correct the dominant asymmetric noise from the remote CNOT and detect the other type of error possibly from

the entanglement swapping process. Note that we can use two of the three logical qubits in each $[[8,3,2]]$ code due to the automorphic structure of the $[[16,6,4]]$ code constructed from the asymmetric $[[8,3,2]]$ pair. We can select larger asymmetric QRM pairs to provide correctability to all types of errors.

VI. Evaluations

We employ asymmetric codes to mitigate the noise introduced by remote CNOTs. For a fixed number of physical qubits in each repeater, we compare our asymmetric code scheme against a baseline in which all repeaters are encoded with identical codes. For the biased noise generated from the remote CNOTs, we assume that the probability of getting a Z error on the control qubit is the same as the probability of getting an X error on the target qubit. We also assume perfect encoders and decoders, with configurable gate noise simulated by depolarizing noise after each intra-repeater gate. In the simulation, we consider 3 repeaters: A, B, and C. We perform entanglement distribution between repeaters A and B, and B and C. Then, we do entanglement swapping inside B. The final logical error rate is calculated based on Bell measurement results of logical qubits in repeaters A and C.

Fig. 9 shows the major results. In the figure, the blue curve uses our new repeater design, where we use different asymmetric $[[8,3,2]]$ codes in neighboring repeaters (two of the three encoded logical qubits are utilized in each code), and the remote CNOTs are used to construct and destruct bigger codes with logical CNOTs done by qubit relabeling. All three other configurations use identical codes in all repeaters, where transversal remote CNOTs are used to implement the logical CNOTs. The orange curve uses identical symmetric $[[8,6,2]]$ codes in all repeaters, and the red curve uses identical symmetric $[[16,6,4]]$ codes in all repeaters. For the green curve, we pick the high d_Z $[[8,3,2]]$ code and use the same code in all repeaters. When there is no gate noise, our asymmetric $[[8,3,2]]$ codes with automorphic CNOTs design achieves a logical error rate as low as that of using identical $[[16,6,4]]$ codes in all repeaters. When the gate noise is $\frac{1}{5}$ of the remote CNOT noise, the logical error rate of our design is even lower than using identical $[[16,6,4]]$ codes. This is also true when the gate noise is $\frac{1}{10}$ or $\frac{1}{2}$ of the remote CNOT noise. Furthermore, our new design always achieves the highest post-selection rate regardless of the gate noise. All results show that our new repeater architecture can achieve a fidelity improvement for a fixed number of physical qubits per repeater.

VII. Conclusion

Remote CNOT protocols employed in entanglement distribution induce asymmetric error patterns, which are not naturally matched to conventional repeater architectures based on identical symmetric quantum error-correcting codes. For asymmetric CSS codes, we showed that both fully and partially transversal logical CNOT approaches impose constraints incompatible with the desired asymmetric protection: stronger Z-error protection on the control side and stronger X-error protection on the target side. Motivated by this, we proposed a repeater architecture that exploits pairs of asymmetric QRM codes together with automorphic logical CNOT gates. The proposed approach temporarily combines neighboring asymmetric code blocks implemented in adjacent repeaters into a larger code using remote transversal CNOT operations. Within the resulting larger code, logical CNOT gates are implemented entirely through local qubit relabelings. This approach avoids the restrictive CNOT transversality requirements of using asymmetric codes in neighboring repeater stations in [4] while simultaneously tailoring the error protection capability of each station to the dominant local noise.

To show the feasibility of our work, we constructed explicit examples based on asymmetric $[[2,1,1]]$ and $[[8,3,2]]$ QRM code pairs. Simulations show that the proposed architecture improves the fidelity of the generated long-distance entanglement compared with conventional designs that employ identical codes at all repeater stations. For a fixed number of physical qubits per repeater, our design achieves lower logical error rates while maintaining higher post-selection rates over a wide range of remote CNOT error probabilities. This work shows that code automorphisms provide a promising mechanism for implementing fault-tolerant logical operations in distributed quantum networks. Recent work [17] has also highlighted the potential of automorphism-based logical CNOTs to reduce the overhead of logical entangling operations and to enable compiler optimization. One future direction is to develop joint decoding schemes that explicitly exploit the correlated error structure of remote CNOTs. By applying suitable local basis rotations after Bell-pair purification to the entangled photon pair, correlated errors of the form $(Z_A X_B)$ may become the dominant error mechanism between neighboring repeaters [16]. In this regime, neighboring stations could exchange syndrome information and decode jointly. Such an approach may provide stronger protection against correlated inter-repeater errors and further improve the performance.

References

[1] R. Alléaume, C. Branciard, J. Bouda, T. Debuisschert, M. Dianati, N. Gisin, M. Godfrey, P. Grangier, T. Länger, N. Lütkenhaus, C. Monyk, P. Painchault, M. Peev, A. Poppe, T. Pornin, J. Rarity, R. Renner, G. Ribordy, M. Riguidel, L. Salvail, A. Shields, H. Weinfurter, and A. Zeilinger, "Using quantum key distribution for cryptographic purposes," *Theor. Comput. Sci.*, vol. 560, no. P1, p. 62–81, Dec. 2014. [Online]. Available: https://doi.org/10.1016/j.tcs.2014.09.018

[2] A. Barg, N. J. Coble, D. Hangleiter, and C. Kang, "Geometric structure and transversal logic of quantum reed–muller codes," *IEEE Transactions on Information Theory*, vol. 72, no. 1, p. 415–436, Jan. 2026. [Online]. Available: http://dx.doi.org/10.1109/TIT.2025.3592631

[3] D. Barral, F. J. Cardama, G. Díaz-Camacho, D. Faílde, I. F. Llovo, M. Mussa-Juane, J. Vázquez-Pérez, J. Villasuso, C. Piñeiro, N. Costas, J. C. Pichel, T. F. Pena, and A. Gómez, "Review of distributed quantum computing: From single qpu to high performance quantum computing," *Comput. Sci. Rev.*, vol. 57, no. C, Aug. 2025. [Online]. Available: https://doi.org/10.1016/j.cosrev.2025.100747

[4] M. Bayanifar, A. Ashikhmin, D. Jiao, and O. Tirkkonen, "On transversality across two distinct quantum error correction codes for quantum repeaters," 2024. [Online]. Available: https://arxiv.org/abs/2406.00350

[5] C. H. Bennett and G. Brassard, "Quantum cryptography: Public key distribution and coin tossing," *Theoretical Computer Science*, vol. 560, pp. 7–11, 2014, theoretical Aspects of Quantum Cryptography

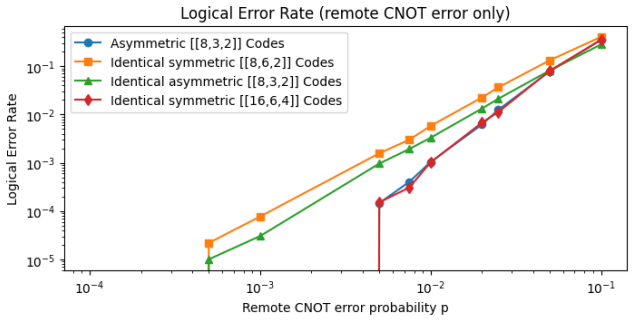

(a) Logical error rates when there is only remote CNOT noise

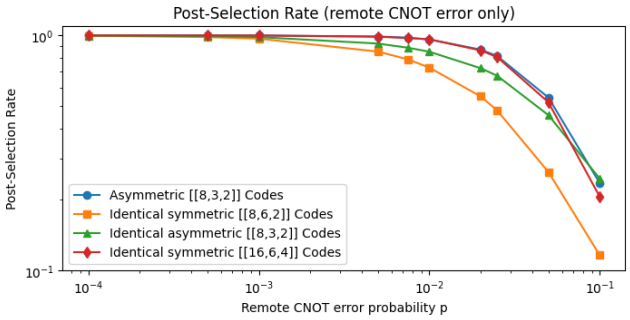

(b) Post-selection rates when there is only remote CNOT noise

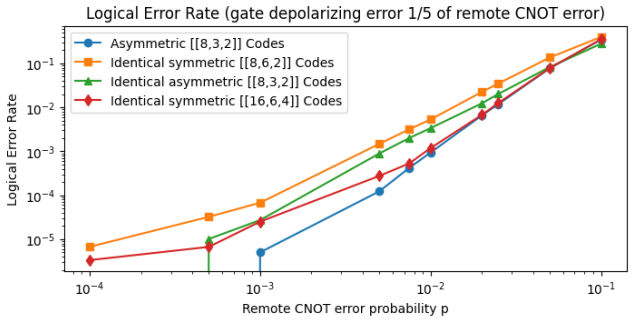

(c) Logical error rates with both remote CNOT and intra-repeater noise

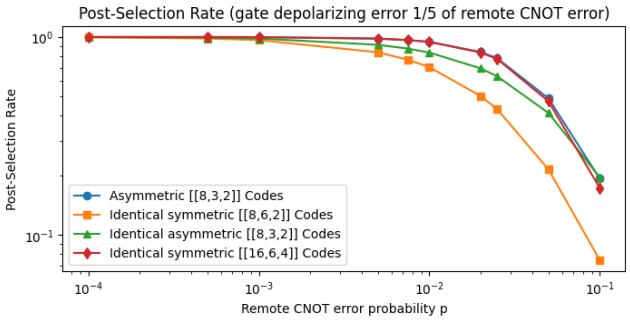

(d) Post-selection rates with both remote CNOT and intra-repeater noise

Fig. 9. Simulation results of logical error rates according to various remote CNOT error probability p across different repeater configurations. (a) and (b) assume only the remote CNOT noise without intra-repeater gate noise. (c) and (d) assume both the remote CNOT noise and intra-repeater gate noise, where the probability of depolarizing error of a gate is $\frac{1}{5}p$ for remote CNOT error probability p.

– celebrating 30 years of BB84. [Online]. Available: https://www.sciencedirect.com/science/article/pii/S0304397514004241

[6] C. H. Bennett, G. Brassard, and A. K. Ekert, "Quantum cryptography," *Scientific American*, vol. 267, no. 4, pp. 50–57, 1992. [Online]. Available: http://www.jstor.org/stable/24939253

[7] S. Bose, V. Vedral, and P. L. Knight, "Multiparticle generalization of entanglement swapping," *Physical Review A*, vol. 57, no. 2, p. 822–829, Feb. 1998. [Online]. Available: http://dx.doi.org/10.1103/PhysRevA.57.822

[8] H. J. Briegel, W. Dür, J. I. Cirac, and P. Zoller, "Quantum repeaters for communication," 1998. [Online]. Available: https://arxiv.org/abs/quant-ph/9803056

[9] A. R. Calderbank and P. W. Shor, "Good quantum error-correcting codes exist," *Physical Review A*, vol. 54, no. 2, p. 1098–1105, Aug. 1996. [Online]. Available: http://dx.doi.org/10.1103/PhysRevA.54.1098

[10] W. Dür, H.-J. Briegel, J. I. Cirac, and P. Zoller, "Quantum repeaters based on entanglement purification," *Phys. Rev. A*, vol. 59, pp. 169–181, Jan 1999. [Online]. Available: https://link.aps.org/doi/10.1103/PhysRevA.59.169

[11] A. K. Ekert, "Quantum cryptography based on bell's theorem," *Phys. Rev. Lett.*, vol. 67, pp. 661–663, Aug 1991. [Online]. Available: https://link.aps.org/doi/10.1103/PhysRevLett.67.661

[12] F. Gaitan, *Quantum Error Correction and Fault Tolerant Quantum Computing*. USA: CRC Press, Inc., 2007.

[13] D. Gottesman, "Stabilizer codes and quantum error correction," 1997. [Online]. Available: https://arxiv.org/abs/quant-ph/9705052

[14] ——, "An introduction to quantum error correction and fault-tolerant quantum computation," in *Quantum information science and its contributions to mathematics, Proceedings of Symposia in Applied Mathematics*, vol. 68, 2010, pp. 13–58.

[15] D. Jiao, A. Ashikhmin, M. Bayanifar, and O. Tirkkonen, "Using small dimensional quantum error correction codes for high-performance quantum communication," in *GLOBECOM 2023 - 2023 IEEE Global Communications Conference*, 2023, pp. 1387–1392.

[16] D. Jiao, M. Bayanifar, A. Ashikhmin, and O. Tirkkonen, " Quantum Error Correction for Second-Generation Quantum Repeaters ," *IEEE Transactions on Quantum Engineering*, vol. 7, no. 01, pp. 1–17, Jan. 2026. [Online]. Available: https://doi.ieeecomputersociety.org/10.1109/TQE.2025.3649561

[17] J. M. Koh, A. Gong, A. C. Diaconu, D. B. Tan, A. A. Geim, M. J. Gullans, N. Y. Yao, M. D. Lukin, and S. Majidy, "Entangling logical qubits without physical operations," 2026. [Online]. Available: https://arxiv.org/abs/2601.20927

[18] S. Muralidharan, L. Li, J. Kim, N. Lütkenhaus, M. D. Lukin, and L. Jiang, "Optimal architectures for long distance quantum communication," *Scientific Reports*, vol. 6, no. 1, Feb. 2016. [Online]. Available: http://dx.doi.org/10.1038/srep20463

[19] J. Preskill, "Reliable quantum computers," *Proceedings: Mathematical, Physical and Engineering Sciences*, vol. 454, no. 1969, pp. 385–410, 1998. [Online]. Available: http://www.jstor.org/stable/53172

[20] A. Steane, "Multiple-particle interference and quantum error correction," *Proceedings of the Royal Society of London. Series A: Mathematical, Physical and Engineering Sciences*, vol. 452, no. 1954, pp. 2551–2577, 1996.

[21] A. M. Steane, "Quantum reed-muller codes," *IEEE Trans. Inf. Theory*, vol. 45, pp. 1701–1703, 1996. [Online]. Available: https://api.semanticscholar.org/CorpusID:15336159

[22] M. Takeoka, S. Guha, and M. M. Wilde, "Fundamental rate-loss tradeoff for optical quantum key distribution," *Nature Communications*, vol. 5, no. 1, Oct. 2014. [Online]. Available: http://dx.doi.org/10.1038/ncomms6235

[23] B. M. Terhal, "Quantum error correction for quantum memories," *Rev. Mod. Phys.*, vol. 87, pp. 307–346, Apr 2015. [Online]. Available: https://link.aps.org/doi/10.1103/RevModPhys.87.307

[24] L. Valentini, R. B. Christensen, P. Popovski, and M. Chiani, "Reliable quantum communications based on asymmetry in distillation and coding," *IEEE Transactions on Quantum Engineering*, vol. 5, pp. 1–13, 2024.

[25] L. Zhang and I. Fuss, "Quantum Reed-Muller codes," 3 1997.